Real-time Conjunction Assessment and Collision Avoidance of Satellites for Concurrent Avoidance Negotiation with Comparative Analysis of Passive Ranging Method and Traditional Sources

Shawn SH Choi[1], Jun Young Byun[2], Maxime Pognon[3], Juhwan Kim[2], Hyeonggu Kim[4], Jaedong Seong[4], Baptiste Guillot[3], Thierry Balanche[3], Kevin Choi[4], Misoon Mah[5], Jae Wook Song[2], Peter JH Ryu[1], Douglas DS Kim[1*]

[1] *SpaceMap Inc. & Voronoi Diagram Research Center, Hanyang University, Korea*
[2] *Department of Industrial Engineering, Hanyang University, Seoul, Korea*
[3] *Satellite Communication & Situational Awareness, Safran Data Systems, France*
[4] *KT SAT, Korea*
[5] *SSA Research Office, Korea Aerospace Research Institute (KARI), Daejeon, Korea*
[6] *M&K Research and Development Inc., VA 20155, USA*

**Corresponding author(douglas.kim@spacemap42.com)*

Abstract

As Geospace becomes more crowded, spacecraft encounter conjunctions more frequently with a higher probability of collision. Human-rated missions are becoming more frequent. Therefore, it is necessary to perform the conjunction assessment (CA) accurately and quickly. Then, the collision-avoidance (COLA) maneuver trajectory, hopefully together with an optimality measure, should be presented as quickly as possible for conjunctions with a sufficiently high probability of collision. However, it is challenging to perform accurate CA/COLA in (near) real-time with the anticipated O(10^6) objects in the space catalogue of the near future. Here we report a rigorous case study on the efficiency and accuracy of the Space-Track TLE database compared to three sources of data: (i) the CDM issued by the US Space Force, (ii) Safran, and (iii) KT SAT. The target objects are GEO satellites. Our observation reconfirms the following but with a new interpretation: (a) The Space-Track TLE data is good and consistent with the CDM; (b) The latency of TLE is significant and should be accounted for as much as possible. A new interpretation: If the TLE data is carefully used, it is useful and consistently close to CDM. In this regard, (i) we introduce the Voronoi-based algorithms for real-time CA and near real-time COLA with the consideration of tertiary conjunctions; (ii) We introduce an architecture of a virtual meeting platform that can be used for the concurrent avoidance negotiation (CAN) of collision situations among involved parties in near real-time; (iii) We introduce an algorithm to detect satellite maneuver quickly and accurately using the TLE data.

Keywords

Real-time, Conjunction Data Message, TLE, Concurrent Avoidance Negotiation, Maneuver Detection, Virtual Meeting, Platform, Voronoi

1. Introduction

Geospace will become rapidly more crowded. This will increase the collision risk between satellites and between satellites and debris. The space catalogue will soon contain O(10^6) or more resident space objects (RSOs), i.e., two orders of magnitude larger than the current O(10^4) size. This is because of (i) evolving measurement systems with advanced sensor technology, (ii) more satellites to be deployed, (iii) Kessler syndrome, etc. The SINTRA project by IARPA is a good example [1]. A recent article reported more than one million (paper) satellites are in the queue of ITU for spectrum [2]. The increasing number of new space situational awareness (SSA) companies, either ground-based or space-based, will altogether contribute to the space catalogue with both higher quality and quantity.

On the other hand, space business requires faster, if not in real-time, solutions to CA/COLA. This is because there will be (i) exponentially more collision-avoiding maneuvers as there are more RSOs, (ii) more human-on-board missions including space tours, (iii) many space planes for intercontinental transportation of freights and passengers that will supplement airplanes if not replace them, etc. In addition, (iv) new applications in the New Space Age will require solving computationally more demanding problems, e.g., optimization and intelligence problems, involving many satellites. Note that a conjunction is an event between two objects. These altogether require accurate and fast solutions to decision-making problems about safety, efficiency, and intelligence in space.

However, these factors overwhelm the capabilities of existing algorithms which have been successful in existing computer programs. The 1984 three-filter algorithm is a good example [3]. Due to this reason in part, emails and phones have been seemingly the only available methods of communication between the parties involved in a **situation-of-interest (SOI)**, e.g., conjunction, when the US Space Force sends out a red-alarm. It was the case in the 2021 Starlink and OneWeb collision [4] and is still the same today. We are not aware of any tool (i) to share SOI with synchronized visualization, (ii) possibly to exchange the state vectors of involved spacecraft, (iii) to generate and evaluate the SOI avoiding alternatives considering involved spacecraft, and (iv) to exchange different perspectives from involved parties. The step (i) can be done through ordinary virtual meeting tools; (ii) requires building a protocol in community – This will be done if it justifies itself; (iii) requires a real-time algorithm for CA/COLA with consideration of tertiary conjunctions – This is the challenge; (iv) can be easily done if the capability (iii) is available.

Here, starting with a brief explanation of an algorithm for real-time CA and COLA, we propose (a) an architecture of concurrent avoidance negotiation (CAN) platform for a SOI with an example, (b) an evaluation of the accuracy of the Space-Track TLE data comparing with another, e.g., passive ranging SSA data, and (c) an algorithm to detect satellite maneuvers. The Astro-1 algorithm is based on Voronoi diagrams and responses to CA queries in real-time and COLA queries in near real-time on a moderate computational platform. Being application-independent, Voronoi diagrams can be used for efficiently solving not only CA/COLA queries, but also optimization problems. Its idea was introduced in AMOS2017 [5] and is publicly available as AstroLibrary [6].

First, we propose an architecture of CAN-platform that uses web links, like a link of GoogleMaps. The CA algorithm first produces and sends conjunction data message (CDM) of SOI to involved parties with a link to its definition. Then, clicking the link should quickly download the platform with the conjunction data to a local device, either laptop or mobile phone. The involved parties should be able to real-time communicate through texts, voices, and videos. All participants must share a synchronized visualization of conjunction. This feature is called "concurrent" "avoidance" "negotiation" because avoidance maneuver alternatives can be created and evaluated concurrently in near real-time, with the consideration of tertiary conjunctions caused by new RSOs beyond the primary and secondary ones. We saw in 2021 [4], there is currently no hard rule to decide who is more responsible about a possible catastrophic event in the timeline – both should negotiate for a reasonable solution of a SOI. It is important that the optimality of avoidance between involved parties is frequently defined with terms beyond technical issues. To reach a solution, both parties should comprehend the situation correctly and quickly. This requires both parties to instantaneously share the ephemeris data of both spacecrafts. This is because the state vector of opponent's spacecraft, available from the databases such as Space-Track and other commercial entities, must have a latency. Given the ephemeris data, the CA algorithm should generate and evaluate collision avoidance maneuver trajectory alternatives for both parties in real-time so that they CAN-communicate to reach a consensus. We believe that these capabilities of a virtual meeting platform are required to promote space industry beyond using emails and phone calls at critical moments. This feature will be indispensable for conflict resolution in global space traffic management or coordination, e.g. TraCSS being developed by the Office of Space Commerce, Department of Commerce. The 2021-like events will be more frequent as mega-constellations, e.g., Kuiper, are being prepared: "Concurrent negotiation" will have to be required!

Second, we present a study on the accuracy of CA because it is important to minimize false alarms for maneuvering. It is well-known that Starlink makes more collision avoidance maneuvers as its constellation grows. In fact, it was shown that the maneuver frequency follows a weakly exponential relationship to satellite count [7]. This observation suggests two issues. (A) Minimizing false alarms is important for keeping satellites longer. (B) The consequence of a maneuver on other maneuvers in the timeline seems to be random. This implies that maneuver generation might be a stochastic process that possesses the memoryless property. These observations suggest the following issues that need to be carefully studied: (a) Increasing the accuracy of SSA data; (b) Reducing the latency of catalogue-update. Here, we present a study on the quality of Space-Track TLE data through a comparative analysis using data from four sources: (i) Space-Track TLE data, (ii) the passive radio-frequency data from SAFRAN, (iii) the ranging data of three primary GEO satellites of KTSAT, and (iv) the US Space Force CDM that is computed using the high accuracy catalogue (HAC) [8].

Third, we present an algorithm based on time series analysis to detect satellite maneuver using the Space-Track TLE data. This is important because latency of the TLE data is one of the most critical factors to its accuracy.

We make the following observations from this study: The Space-Track TLE data is consistent with the CDM from the US Space Force; The Space-Track TLE data can be more useful if the latency between measurement and cataloguing can be appropriately accounted for; The latency-reflected Space-Track TLE data shows accuracy close to commercial SSA data; The Space-Track TLE database is updated more frequently than we first thought; The real-value of commercial SSA data might be tracking the secondary satellite; Early detection of maneuver is important for making the Space-Track TLE data more valuable; There should be a playground for sharing satellites' ephemeris data.

Section 2 briefly describes the real-time CA and near real-time COLA algorithms. Section 3 introduces the architecture of the virtual meeting platform that can be used for concurrent avoidance negotiation for a conjunction situation. This section also shows an example called "42 Talks." Section 4 describes the experimental setting. Section 5 describes the experiment to compare CDMs with the conjunctions computed using databases. Section 6 presents a maneuver detection algorithm. Section 7 concludes.

2. Real-time Conjunction Assessment and Collision-Avoidance

Astro-1 has SaaS services for real-time CA and near real-time COLA using the Space-Track TLE database. Given the input TLE data, it creates a preprocessing database called the proximity database **ProxiDB** which stores critical space-time events of moving RSOs. These events are identified from the dynamic Voronoi diagram of the moving RSOs. Given a ProxiDB, queries for CA/COLA can be answered fast by scanning a subset of ProxiDB to find solutions. Note that Voronoi diagrams are well-known as the most compact data structure for spatial reasoning among particles. Dynamic Voronoi diagrams are their counterparts for moving particles and was introduced for CA in AMOS2017. It turns out useful not only for CA/COLA but also for computationally more challenging optimization problems. See [5, 6].

The solution produced by Astro-1 is associated with an error which consists of three major terms related to (i) algorithmic correctness, (ii) the latency between the measurement and database cataloging, and (iii) measurement uncertainty. We have verified the correctness of the algorithms from both theoretical and experimental points of view. We have repeatedly confirmed that the Astro-1 solutions and those from STK are practically and statistically identical for the same data sets.

The latency issue is of importance and interest in this study. Regardless of their types, SSA databases inevitably have latency. In other words, there exists a time lag between the moment an object is measured and the moment its state vector is populated/catalogued in a space catalogue. Latency can be minutes, hours, or days. Because a space object may change its state vector at any moment, latency can be critical for making the right judgement about the state of an object. For example, if an object starts to maneuver immediately after it was measured, and if its state vector is catalogued in a database after one hour, the actual state of the object and the state that is stored in the database can be significantly different. Therefore, a judgement based on the catalogue should be made carefully. A judgement can be either cooperative or competitive. One of the purposes of the experiment in this study is to evaluate the significance of the latency of the Space-Track TLE data for CA. The third term, i.e., measurement uncertainty, is not discussed in this study.

3. Virtual Meeting Platform for Concurrent Avoidance Negotiation

The prediction of future state of a space object and the prediction of future state of a space-time event that involves two or more space objects are important for both commercial and national security purposes. For example, consider if a conjunction is predicted using a CA algorithm and a space catalogue, say the Space-Track TLE database, between two satellites where each belongs to different space entities, say A and B. Depending on when the measurements were made, when the orbit data was catalogued in the database, and when the TLE data was downloaded from the database, the discrepancy between the actual distance and modelling distance between A and B satellites can be large. Regardless of the databases, e.g., Space-Track TLE or HAC, commercial SSA companies, etc., there exists a latency, from minutes to sometimes hours. A red alert warning can be a false alarm due to the discrepancy.

We observe that the latency of trajectory data is inevitable and can be critical in a conjunction situation. The best way to get away from this issue is to share trajectory data, usually in ephemeris format that is a series of time-stamped waypoints, between parties involved in a conjunction. With ephemeris data, each of the involved parties can generate and evaluate alternatives to find the best option from each individual perspective. It might be necessary for them to communicate to negotiate because involved parties might have different opinions about conjunction avoidance. Depending on situation, they would wish to evaluate alternatives in real-time on the fly. However, it is current practice that the involved parties communicate using emails and phone calls. In the 2021-conjunction between Starlink and OneWeb [4], they also used emails and phone calls.

In this regard, we propose the capabilities and architecture of a virtual meeting platform where participants can be invited to share any space-situations including conjunctions and exchange different perspectives. It has the capability for visualizing space-situations in addition to most standard features of a virtual meeting platform such as Google Meet and Zoom. Participants can communicate using texts, voices, and videos and can have a virtual presentation session. It is also important for this platform to have a **concurrent avoidance negotiation (CAN)** capability. Participants can generate and evaluate trajectory alternatives in real-time with respect to some measures, e.g., collision risks. Then, they can exchange opinions to find mutually agreeable solutions.

Fig. 1(a) depicts the schematic diagram of the procedure of such a platform. A meeting organizer sends out an invitation with a CDM link that stores the space-situation information to involved parties. Then, by clicking the link, each recipient downloads and runs the platform. In this example, the organizer calls for a meeting with a CDM-link sent to the catalogued social media of participants, say, Stalink and OneWeb, after predicting a conjunction. Then, by clicking the link, Starlink and OneWeb may immediately join the meeting through the platform or may schedule a meeting. While they exchange ideas to resolve the conjunction, they may generate and evaluate maneuver alternatives and negotiate for a collision avoidance maneuver that both agree upon. All these should be done near real-time in the platform.

Fig. 1(b) shows such an example of virtual platform called "42 Talks" (platform.spacemap42.com) developed by SpaceMap: Five participants at the top of the window, a space-situation of conjunction, and a chatting window to the right. The conjunction situation in the center of the window is actually synchronized among participants. An individual with a handle can manipulate the visualization to lead a conversation and can pass it over another individual. The chatting window shows that some participants are communicating through texts. If necessary, the participants for each of the orange and violet satellites can individually generate and evaluate maneuver alternatives. Then, they can negotiate for a resolution. Participants may be cooperative or competitive.

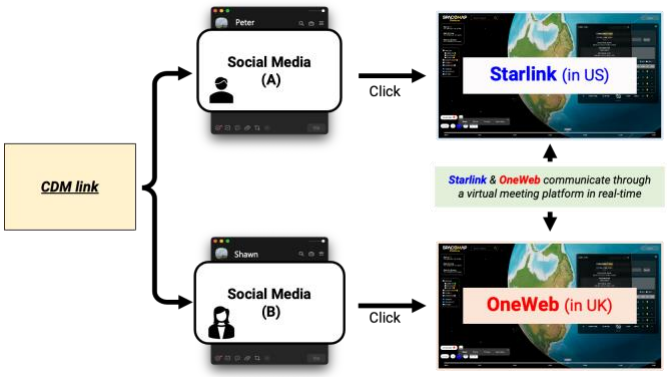

(a)

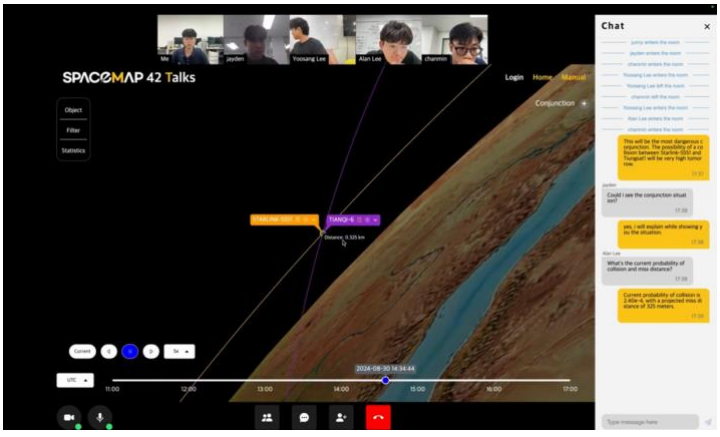

(b)

Fig. 1 A proposal of virtual meeting platform for SSA and STM. (a) The flow of the user interaction logic. (b) An example of the virtual platform "42 Talks." Five participants are shown on the top of the platform. A conjunction situation is 3D visualized in the timeline. Communication is done through the texts in the chatting window in the right.

4. Experimental Settings

We conducted a comparative experiment using the following data: (i) CDM from the USSF, (ii) Space-Track TLE database, (iii) Safran Data Systems WeTrack database, (iv) the ephemeris data of a satellite of KT SAT, and (v) the CA results from Astro-1. The scenario: First, we chose a primary satellite with ephemeris data for a confirmed trajectory. We chose the target which had received CDMs from the US Space Force (SF). It is known that CDM is produced using HAC that is maintained by the USSF [8]. We chose KOREASAT 5A (NORAD ID: 42984), abbreviated as K5A, of KT SAT's GEO telecommunication satellite, as the primary. K5A performed maneuvers regularly for accurate repositioning and the corresponding ephemeris data is archived. We used two CDMs for K5A as the ground-truth values and the WeTrack data of Safran Data System for the benchmark with the Space-Track TLE data. For the state vector of the secondary satellite, we used the Space-Track TLE database. With the state vectors of a satellite pair (primary, secondary), we used Astro-1 to do the CA during the experiment time window.

Safran WeTrack System

Safran has a ten-year old passive RF sensor network, WeTrack, for geosynchronous spacecrafts. Passive RF allows for weather-independent diurnal and nocturnal measurements, individual spacecraft identification, spacecraft RF behavior characterization, etc. WeTrack relies on Time Difference of Arrival (TDOA) and Frequency Difference of Arrival (FDOA) measurements of spacecrafts for accurate orbit determination. The Cross-Ambiguity Function (CAF) of two different RF signals collected on two distant Earth stations (separated by about 300km) is used to measure TDOA and FDOA values. A minimum sensor architecture is made of three ground stations. High accuracy time and frequency sensor synchronization is achieved using GNSS constellations (GPS & GALILEO). All the stations of a cluster are pointing synchronously toward the same target to perform the acquisition of the signal of interest. Acquired signal snapshots are transferred to computer form the CAF estimation to determine the target's TDOA & FDOA. Fig. 2(a) and (b) show the Safran WeTrack system.

KT SAT Groundstations

KT SAT, a subsidiary of Korea Telecom, owns/operates five GEO satellites to provide satcom services for civil, government, maritime customers, etc. In this study, KT SAT provided actual measurement data, performed on K5A. KT SAT performs ranging operation by using antennas located in two different sites in South Korea. KT SAT owned antennas are equipped with Monopulse Tracking Systems (MTS) which is known to provide high accuracy with real-time error calibration. The ranging data from each antenna is used separately for the Orbit Determination (OD) due to distance constraint between two antenna sites. Azimuth and elevation data are obtained by tracking the satellite's beacon signal using the Monopulse system. The range data is derived by measuring the time taken for a signal sent from the ground baseband equipment to travel to the satellite and back. Forty-eight sets of azimuth, elevation, and range data are used in the OD process in every one-hour interval. Fig. 1(c) and (d) show the KT SAT antenna system.

(a) (b) (c) (d)

Fig. 2. Databases used. (a) and (b) Safran's WeTrack system: The schematic of system architecture; The antennas. (c) and (d) KT SAT TM & TC Antenna Farm: KT SAT Ranging Signal Flow

5. Comparison: CDM vs. Conjunctions Computed using Space Databases

We performed an experiment to understand the latency term of error as follows. We used two CDM data for KOREASAT 5A (NORAD ID: 42984), abbreviated as K5A from the USSF 18 SDS as the reference: CDM#1 and CDM#2. We used Astro-1 for the computation of DCA/TCA. We used the databases as follows: For the primary satellite K5A, we used Space-Track TLE, Safran WeTrack, and KT SAT ephemeris; For the secondary satellite, the Space-Track TLE database was used. UTC is the time unit used unless otherwise stated.

CDM#1

CDM#1 was created at 12:53:21 and received by KT SAT at $T_{receive}$ = 15:00:00, both on 2023-09-28. The secondary was Elektro–L (NORAD ID: 37344) operated by Roskosmos. TCA_{CDM} defined by CDM was 20: 09:39 on 2023-09-29 with DCA_{CDM} of 4.382km. TCA_{CDM} was about 29 hours after the time $T_{receive}$. Let DAY^{CDM} be the date containing TCA_{CDM} and $DAY^{CDM\text{-}x}$ the x-days before DAY^{CDM}: i.e., $DAY^{CDM\text{-}2}$ = Sep 27, $DAY^{CDM\text{-}1}$ = Sep 28, and DAY^{CDM} = Sep 29. K5A maneuvered at 10:00:00 Sep 27.

We compared CDM#1 with other SSA data over three days as follows. Let CA3 be the CA for DAY^{CDM} computed at 00:00:00 on DAY^{CDM} using the best-available data. CA2 corresponds to the CA for DAY^{CDM} computed at 00:00:00 on $DAY^{CDM\text{-}1}$ using the best-available data. Likewise, CA1 corresponds to $DAY^{CDM\text{-}2}$. The best-available data means the most-recently updated data that was downloaded. Let TLE1, TLE2, and TLE3 denote the TLE data used for CA1, CA2, and CA3, respectively. We distinguish three instances for TLE: (i) the moment of orbit determination using measurement (called as **epoch time**), (ii) the moment of cataloging in the Space-Track TLE database (called as **creation time**), and (iii) the moment we download the TLE data from Space-Track (called as **receiving time** $T_{receive}$).

Fig. 3 shows the eccentricity and semi-major axis of the K5A orbit represented in the Space-Track TLE data. The data was downloaded and evaluated every hour on the hour during the 72-hour **experiment window** between 00:00:00 Sep 26 and 00:00:00 Sep 30. The intervals corresponding to the non-horizontal line segments contain the creation time of the K5A TLE data. The rectangles and triangles correspond to epoch and creation times, respectively. The additional three dotted vertical lines correspond to the moments of the CA1, CA2, and CA3 computation. The blue and red denote before and after of the K5A maneuver. Note that the maneuver was reflected in the TLE3 file used for the CA3 computation: It was downloaded immediately after the update which had caused a big change of semi-major axis. The black triangles correspond to the West-bound maneuver of K5A at 10:00:00 2023-09-27: East-West maneuver influences eccentricity and semi-major axis. The yellow rectangles denote CDM.

Fig. 4 shows the chronological events of data items. The horizontal line denotes the timeline. The eight numbered boxes with white background correspond to the data representations of the primary and secondary objects: The boxes are ordered from 1 to 8 in the timeline: The primary above the time axis and the secondary below. The small green rectangles attached to the boxes denote the CA computations that the data was used. The black ellipse denotes the West-bound maneuver of K5A; Its ephemeris became immediately available at this moment. The rounded capsules denote the computations of CA1, CA2, and CA3. The five boxes left of and the two right of the maneuver are blue- and red-colored, respectively. WeTrack had only one version of the K5A data during the entire experiment with the epoch time 11:17:24 2023-09-12.

The TLE data of the primary and secondary was updated four and five times during the 48-hour period between 00:00:00 Sep 27 and 00:00:00 Sep 29, respectively. We observed that CDM was generated after the maneuver, probably using the HAC data created before the maneuver of K5A. Data set used for the CA1 computation: Boxes 1, 2, and 3; those for CA2: 1, 4, 5, and 6; those for CA3: 1, 6, 7, and 8. TLE3 is the only updated available data after the maneuver, except the K5A's ephemeris.

Table 1 summarizes statistics. In CA1, (primary = TLE1, secondary = TLE) showed ΔDCA = - 0.255km which denotes the DCA computed by Astro-1 subtracted by the DCA in CDM. The corresponding (Safran, TLE) produced ΔDCA = 8.387km. KT SAT data was not available at this time. In CA2, (TLE2, TLE) showed ΔDCA = - 0.229km: The small difference |0.255 – 0.229| might be due to the tiny difference in the TLE data of the primary and secondary. (Safran, TLE) showed ΔDCA = 8.543km; The difference | 8.387 - 8.543 | seems due to the variation in the TLE data because the Safran data did not change during the experiment window. (KT SAT, TLE) showed ΔDCA = 30.241km using the K5A's ephemeris data after the maneuver. In CA3, (TLE3, TLE) showed ΔDCA = 27.641km. Observe that TLE3 reflected the maneuver. (Safran, TLE) showed ΔDCA = 7.128km. (KT SAT, TLE) showed ΔDCA = 28.898km using the ephemeris data.

Observe that the small difference | 27.641 - 28.898 | implies that the Space-Track TLE data became consistent with the actual K5A maneuver. We concluded that the HAC counterpart would have been more consistent with the K5A maneuver, and it was not necessary for the USSF to send out another CDM to KT SAT.

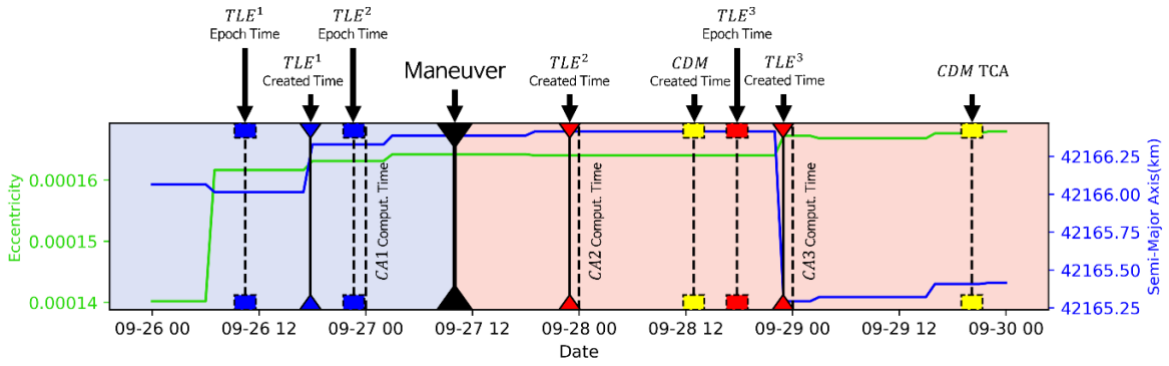

Fig. 3. Eccentricity and semi-major axis represented in the Space-Track TLE data of KOREASAT 5A (K5A, 42984). The secondary was Elektro–L (NORAD ID: 37344). Eccentricity in green and semi-major axis in blue. Between Sep 26 and 30 (i.e. 72 hours), the K5A TLE data was downloaded and evaluated every hour on the hour. The rectangles and triangles correspond to epoch and creation times of the K5A TLE data. The blue and red denote before and after the maneuver. The black triangles correspond to the maneuver of K5A. The additional three dotted vertical lines correspond to the moments of the CA1, CA2, and CA3 computation. CDM was created after the maneuver, believably using the HAC data measured before the maneuver.

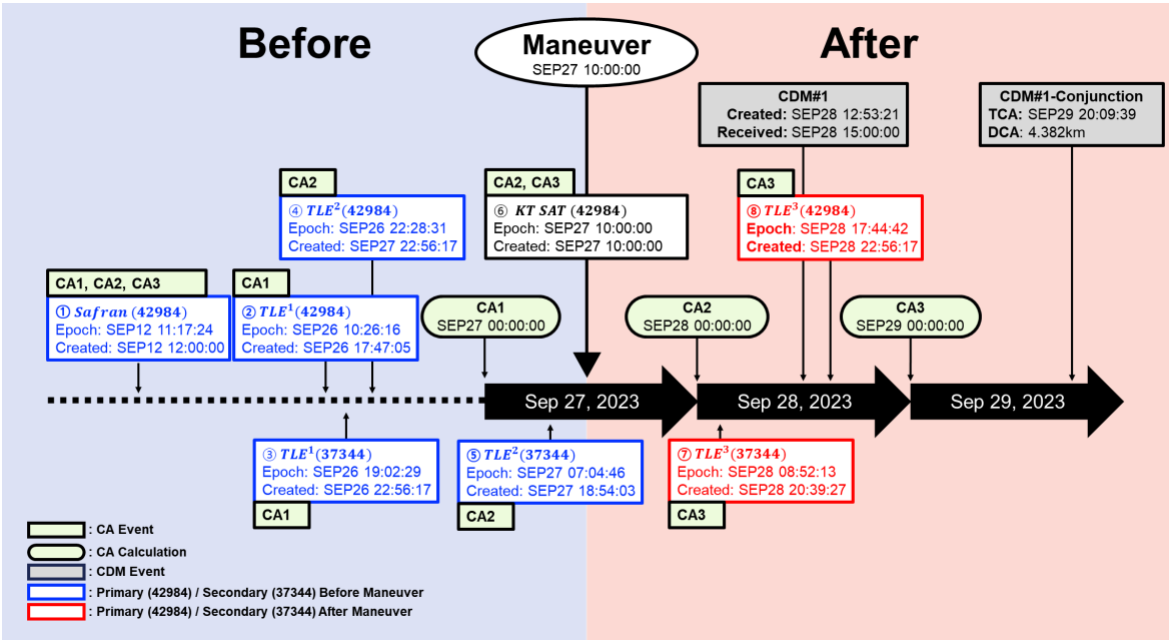

Fig. 4. CDM#1 and the three CAs using other databases. Three databases were used: Space-Track TLE, Safran WeTrack, and KT SAT ephemeris. The eight numbered boxes with white background correspond to the data representations of the primary and secondary objects. The black ellipse denotes the West-bound maneuver of K5A. The rounded capsules denote the computations of CA1, CA2, and CA3. We observed that CDM was generated after the maneuver.

Table 1 CDM#1 and the output of the benchmark test with the Space-Track TLE and Safran WeTrack databases compared with the KT SAT K5A satellite ephemeris data. Three CA sets used: CA1, CA2, and CA3. KT SAT data was not available for CA1. Δ denotes an Astro-1 value subtracted by the corresponding CDM value, i.e., $\Delta = \text{Astro1} - CDM$. All computations were done using Astro-1.

CA1 (CDM#1) @ SEP27, 2023 00:00:00	**Database Type**	TLE	Safran	KT SAT
	Primary: 42984	Epoch time @ SEP26 10:26:16 (Before Maneuver)	Epoch time @ SEP12 11:17:24 (Before Maneuver)	Epoch time : N/A
	Secondary: 37344	TLE epoch@ SEP26 19:02:29		
	TCA	SEP29 20:09:49	SEP29 20:09:00	N/A
	ΔTCA (seconds)	+10 seconds	-39 seconds	N/A
	DCA (km)	4.127km	12.769km	N/A
	ΔDCA (km)	- 0.255km	+8.387km	N/A
CA2 (CDM#1) @ SEP28, 2023 00:00:00	**Database Type**	TLE	Safran	KT SAT
	Primary: 42984	Epoch time @ SEP 26 22:28:31 (Before Maneuver)	Epoch time @ SEP12 11:17:24 (Before Maneuver)	Epoch time @ SEP27 10:00:00 (After Maneuver)
	Secondary: 37344	TLE epoch@09-27T18:54:03		
	TCA	SEP29 20:09:49	SEP 29 20:09:00	SEP 29 20:09:37
	ΔTCA (seconds)	+10 seconds	-39 seconds	-2 seconds
	DCA (km)	4.153km	12.925km	34.623km
	ΔDCA (km)	-0.229km	+8.543km	+30.241km
CA3 (CDM#1) @ SEP29, 2023 00:00:00	**Database Type**	TLE	Safran	KT SAT
	Primary: 42984	Epoch time @ SEP 28 17:44:42 (After Maneuver)	Epoch time @ SEP 12 11:17:24 (Before Maneuver)	Epoch time @ SEP 27 10:00:00 (After Maneuver)
	Secondary: 37344	TLE epoch@09-28T08:52:13		
	TCA	SEP 29 20:09:40	SEP 29 20:09:00	SEP 29 20:09:37
	ΔTCA (seconds)	+1 seconds	-39 seconds	-2 seconds
	DCA (km)	31.813km	11.51km	33.28km
	ΔDCA (km)	+27.641km	+7.128km	+28.898km

Fig. 5 shows three clusters of relatively similar DCA values. The three DCAs in the red elliptic cluster were computed using the primary satellite data represented by either the K5A ephemeris data or the Space-Track TLE data which was measured and orbit-determined after the maneuver. The three DCAs in the blue elliptic cluster were computed using the Space-Track TLE data with orbit-determined before the maneuver. Those in the other cluster were computed using the WeTrack database.

From the CDM#1 experiment, we observe the following.

(i) The CA result using TLE3 is close to that using the K5A ephemeris on Sep 29, i.e., after the maneuver is properly reflected in TLE3.

(ii) CDM and the CA computed using the Space-Track TLE data are consistent and close to each other. Hence, the CA result based on TLE is useful when latency is properly accounted for.

(iii) CDM was not received by KT SAT again for the same conjunction. This would be probably because the DCA was large enough, i.e., >25km, as is indicated by the DCA value of CA3.

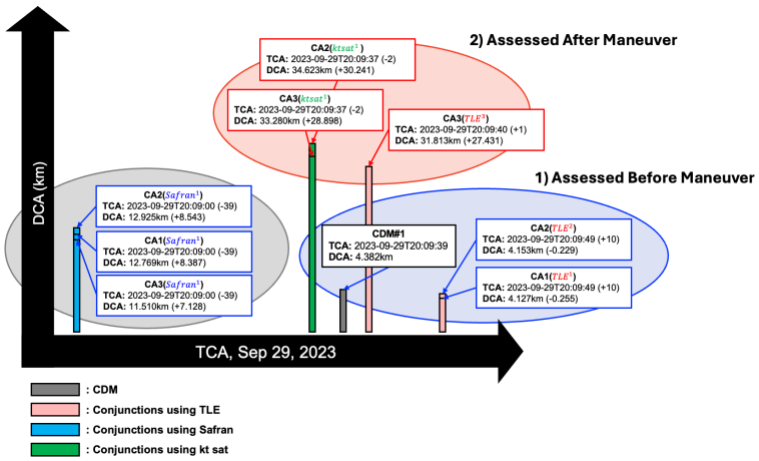

Fig 5. Three clusters of similar DCA values. The red cluster contains three DCAs computed using the primary satellite data represented by either the K5A ephemeris data or the Space-Track TLE data which was measured and orbit-determined after the maneuver. The three DCAs in the blue cluster were computed using the Space-Track TLE data with orbit-determined before the maneuver. The grey cluster were computed using the WeTrack database.

CDM#2

CDM#2 was created at 13:45:05 and received by KT SAT at $T_{receive}$ = 16:05:00, both on 2023-10-14 with (Primary = K5A, Secondary = RADUGA 1-4 (NORAD ID: 25642)). TCA_{CDM} was 15: 26:36 on 2023-10-16 with DCA_{CDM} of 4.930km. TCA_{CDM} was about 48 hours after the time $T_{receive}$. We conducted the benchmark for CDM#2 over four days as follows. Let CA4 be the CA for DAY^{CDM} computed at 00:00:00 on DAY^{CDM} using the best-available data. CA3, CA2, and CA1 correspond to DAY^{CDM-1}, DAY^{CDM-2}, and DAY^{CDM-3}, respectively. The best-available data means the most-recently updated data that was downloaded. Let TLE1, TLE2, TLE3, and TLE4 denote the TLE data used for CA1, CA2, CA3, and CA4, respectively. In the Space-Track TLE database, the primary and secondary were updated ten and eight times, respectively.

CDM#2 was created believably using the HAC data for K5A measured after the maneuver. However, the maneuver was correctly reflected in TLE3 for CA3. Safran showed a consistent result both before and after the maneuver despite that its K5A state vectors were created before the maneuver. The small variation of DCAs for Safran and KT SAT columns are believably due to the variation of the TLE data of the secondary. This implies that the secondary probably did not maneuver. The TLE data of the secondary did not change much during the four-day period.

Fig. 6 shows the eccentricity and semi-major axis represented in the Space-Track TLE data of K5A. Fig. 4 shows the chronological events of data items. Table 1 summarizes statistics. From the analysis similar to CDM#1, we observe the following.

- After the maneuver is reflected, the Space-Track TLE data produces results that are close to CDM.

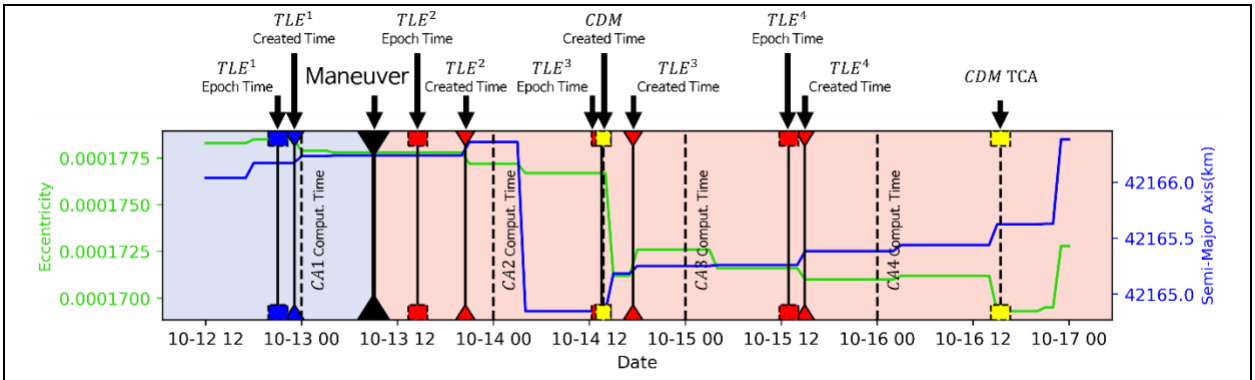

Fig. 6. Eccentricity and semi-major axis represented in the Space-Track TLE data of KOREASAT 5A (K5A, 42984). The secondary was RADUGA 1-4 (NORAD ID: 25642). Eccentricity in green and semi-major axis in blue. Between 12:00:00 Oct 12 and 00:00:00 Oct 17, the K5A TLE data was downloaded and evaluated every hour on the hour. The rectangles and triangles correspond to epoch and creation times of the K5A TLE data. The blue and red denote before and after the maneuver. The black triangles correspond to the maneuver of K5A. The additional four dotted vertical lines correspond to the moments of the CA1, CA2, CA3, and CA4 computation. CDM was created after the maneuver, but believably using the HAC data measured before the maneuver.

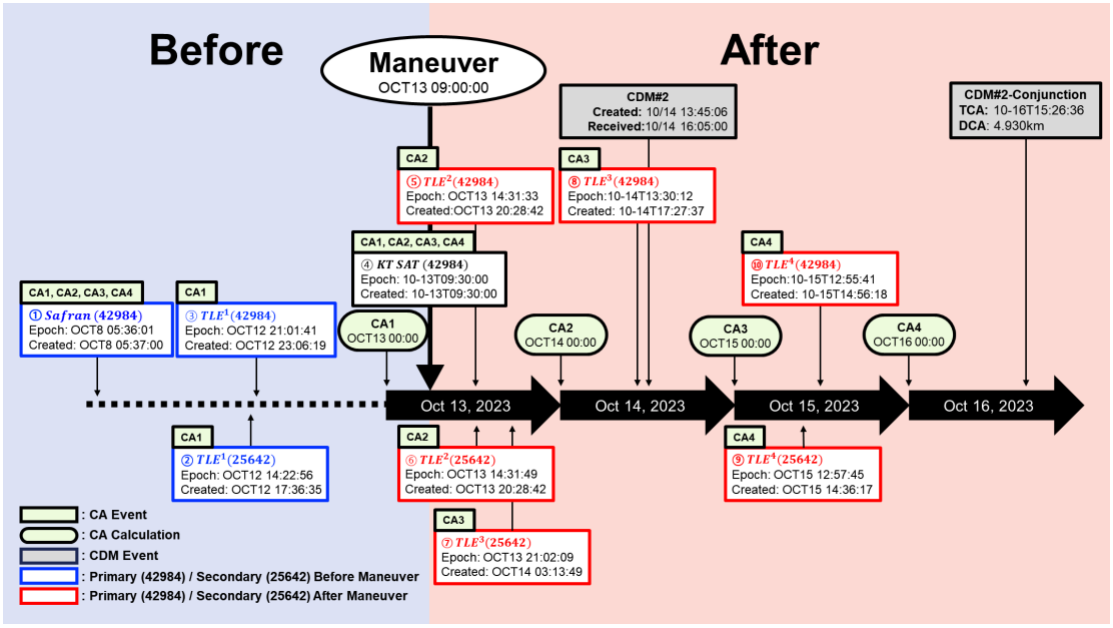

Fig. 7. CDM#2 and the four CAs using other databases. Three databases were used: Space-Track TLE, Safran WeTrack, and KT SAT ephemeris. The ten numbered boxes with white background correspond to the data representations of the primary and secondary objects. The black ellipse denotes the West-bound maneuver of K5A. The rounded capsules denote the computations of CA1, CA2, CA3, and CA4. We observed that CDM was generated after the maneuver.

Table 2 CDM#2 and the output of the benchmark test with the Space-Track TLE and Safran WeTrack databases compared with the KT SAT K5A satellite ephemeris data. Four CA sets used: CA1, CA2, CA3, and CA4. KT SAT data was not available for CA1. Δ denotes an Astro-1 value subtracted by the corresponding CDM value, i.e., $\Delta = \text{Astro1} - CDM$. All computations were done using Astro-1.

CA1 (CDM#2) @ OCT13, 2023 00:00:00	**Database Type**	TLE	Safran	KT SAT
	Primary: 42984	Epoch time @ OCT12 21:01:41 (Before Maneuver)	Epoch time @ OCT08 05:36:01 (Before Maneuver)	N/A
	Secondary: 25642	TLE epoch@OCT12 14:22:56		
	TCA	OCT16 15:26:45	OCT16 15:26:39	N/A
	ΔTCA (seconds)	+10 seconds	+3 seconds	N/A
	DCA (km)	27.589km	9.209km	N/A
	ΔDCA (km)	+22.659km	+4.279km	N/A
CA2 (CDM#2) @ OCT14, 2023 00:00:00	**Database Type**	TLE	Safran	KT SAT
	Primary: 42984	Epoch time @ OCT13 14:31:33 (After Maneuver, unreflected)	Epoch time @ OCT08 05:36:01 (Before Maneuver)	Epoch time @ OCT13 09:30:00 (After Maneuver)
	Secondary: 25642	TLE epoch@ OCT13 14:31:49		
	TCA	OCT16 15:26:45	OCT16 15:26:39	OCT16 15:26:32
	ΔTCA (seconds)	+10 seconds	+3 seconds	-4 seconds
	DCA (km)	28.429km	9.091km	9.708km
	ΔDCA (km)	+23.499km	+4.161km	+4.778km
CA3 (CDM#2) @ OCT15, 2023 00:00:00	**Database Type**	TLE	Safran	KT SAT
	Primary: 42984	Epoch time @ OCT14 13:30:12 (After Maneuver, reflected)	Epoch time @ OCT08 05:36:01 (Before Maneuver)	Epoch time @ OCT13 09:30:00 (After Maneuver)
	Secondary: 25642	TLE epoch@ OCT13 21:02:09		
	TCA	OCT16 15:26:46	OCT16 15:26:39	OCT16 15:26:32
	ΔTCA (seconds)	+11 seconds	+3 seconds	-4 seconds
	DCA (km)	10.442km	9.212km	9.830km
	ΔDCA (km)	+5.512km	+4.282km	+4.900km
CA4 (CDM#2) @ OCT16, 2023 00:00:00	**Database Type**	TLE	Safran	KT SAT
	Primary: 42984	Epoch time @ OCT15 12:55:41 (After Maneuver, reflected)	Epoch time @ OCT08 05:36:01 (Before Maneuver)	Epoch time @ OCT13 09:30:00 (After Maneuver)
	Secondary: 25642	TLE epoch@ OCT15 12:57:45		
	TCA	OCT16 15:26:50	OCT16 15:26:39	OCT16 15:26:32
	ΔTCA (seconds)	+14 seconds	+3 seconds	-4 seconds
	DCA (km)	10.470km	8.809km	9.422km
	ΔDCA (km)	+5.540km	+3.879km	+4.492km

6. Maneuver Detection

The detection of maneuver is important for a better understanding of space situations including CA using the Space-Track TLE data. There are also other reasons related to defense and security for space. Here we report a maneuver detection algorithm with some experimental results.

6.1. The ICCS Algorithm to Detect Station-Keeping Maneuvers in GEO

GEO satellite orbits are affected by various perturbations, causing their inclination, longitude, and eccentricity to drift over time. Station-keeping maneuvers are used to maintain a satellite within its assigned longitude and inclination box [9]. We first tested the proposed maneuver detection algorithm on a GEO satellite's station-keeping maneuvers. To detect maneuvers, we observed changes in the statistical properties of the time series. A change point (CP) occurs when these properties deviate from normality, indicating a structural break. One popular model for identifying structural breaks in time series is the **iterative cumulative sum of squares (ICSS) algorithm** [10]. The ICSS algorithm is popular in various fields including finance [11], energy [12], agriculture [13], etc. We developed a modified ICSS approach to detect CPs in satellite geolocation time series online, identifying maneuver points or significant changes in satellite movement.

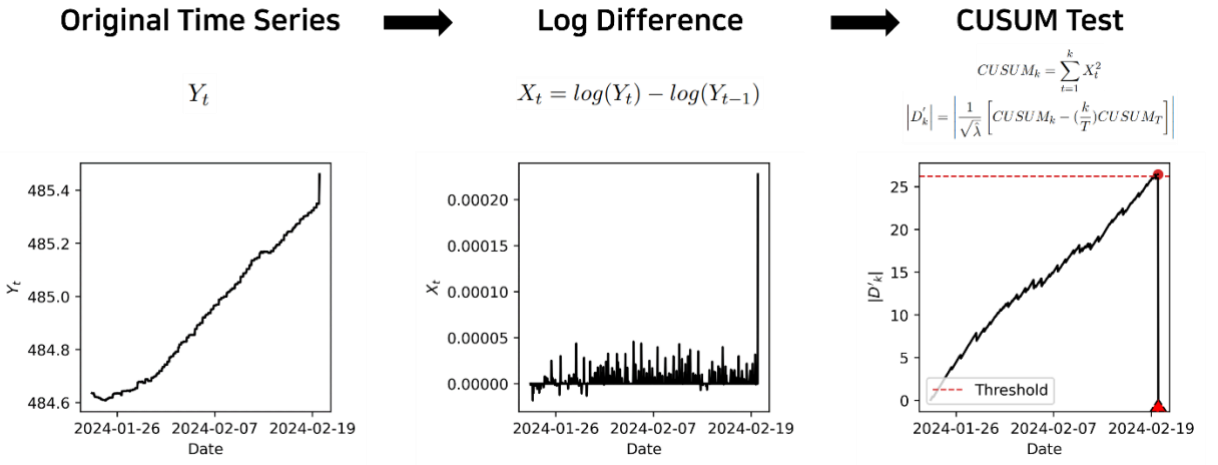

Fig. 8. Idea of maneuver detection using a cumulative sum CUSUM in a time series

Figure 8 illustrates the idea of maneuver detection in timeline using a cumulative sum CUSUM. Let Y_t denote the original time series with T as the series length, $t = 1, 2, \dots, T$. The input data of CUSUM test, X_t, is the log difference of Y_t: $X_t = log(Y_t) - log(Y_{t-1})$ where $X_t = \mu_t + R_t$ where μ_t is the mean, and R_t is the noise with a zero mean. The CUSUM detects the mean change from the start ($t = 1$) to the end ($t = T$) for offline detection. For online detection, testing occurs at each update. The CUSUM can be applied as a non-parametric method for identifying CPs as follows:

$$CUSUM_k = \sum_{t=1}^{k} X_t^2, \qquad k = 1,2,\cdots,T \tag{1}$$

Then, D_k statistics can be calculated as

$$D_k = \frac{CUSUM_k}{CUSUM_T} - \frac{k}{T}, \qquad k = 1,2,\cdots,T \tag{2}$$

where $D_0 = D_T = 0$. Here we use D'_k modified from D_k since the CP estimation using the current D_k fails to account for the substantial kurtosis and conditional heteroskedasticity that deviate from normal distribution [14]. D'_k with the non-parametric statistic using the Bartlett kernel proposed in [11] can be defined as follows:

$$D'_k = \frac{1}{\sqrt{\hat{\lambda}}}\left[CUSUM_k - \left(\frac{k}{T}\right)CUSUM_T\right], \qquad k = 1,2,\cdots,T \tag{3}$$

The threshold for identifying CPs is determined by significance levels at $\alpha = 0.05$ and $\alpha = 0.01$ which correspond to the 95th and 99th percentiles of $|D'_k|$, respectively. Since D'_T is 0, if the value of $|D'_{T-1}|$ exceeds this threshold, the null hypothesis of a constant mean is rejected, and the point is classified as a CP.

The CUSUM test detects CPs in time series data by focusing on the most recent value. It turns out to be effective for the station-keeping maneuvers in GEO and further improvements are expected for detecting continuous maneuvers which involve gradual changes in parameters over time. The moving window size was tested with different durations, e.g., 5 days (120 hours) and 10 days (240 hours).

6.2. Examples of Maneuver Detection

We tested the proposed maneuver detection algorithm for two satellites: KT SAT GEO satellite K5A (NORAD ID: 42984) and MALLIGYONG-1 (NORAD ID: 58400), a North Korean LEO satellite. The TLE data for K5A was extracted for the experiment period from Sep 21 to October 31, 2023; The experiment period of MALLIGYONG-1 was from Nov 22, 2023, to Jul 31, 2024. For both satellites, TLE data was retrieved on an hourly basis, using the most recent data available at each time point.

[K5A] (See Fig. 9 and 10)
During the experiment period, K5A performed three North-South and six East-West, both station-keeping, maneuvers. We compared the results of the TLE-based maneuver detection with the nine actual maneuvers recorded by KT SAT to assess the accuracy of the detection algorithm. The North-South maneuvers were detected by the changes in the inclination and right ascension of the ascending node (RAAN). The East-West ones were detected by the changes in the eccentricity and semi-major axis. We used window sizes of 120 hours and 240 hours, and applied significance levels of 95% and 99%. We observed that when each of inclination, RAAN, eccentricity, and semi-major axis was applied separately, solution resulted in numerous false positives. On the other hand, the intersection of inclination and RAAN for the North-South and the intersection of eccentricity and semi-major axis for the East-West maneuvers produced the best results when 99% significance level was applied to. The algorithm appears to perform well in detecting GEO station-keeping maneuvers using the TLE data. We consider the (240 hours, 99%) pair performs best. It is important to note the inevitable latency between the actual maneuvers and the detected maneuver moments. The additional events detected by the algorithm also deserve further investigation.

[MALLIGYONG-1] (See Fig. 11 and 12)
An experiment similar to the one for the K5A GEO satellite was performed for the MALLIGYONG-1 LEO satellite. Specifically, calculations for both Out-of-Plane (corresponding to North-South for GEO) and In-Plane (corresponding to East-West for GEO) maneuvers were carried out. However, unlike K5A, there does not exist any reference data (true values) available for MALLIGYONG-1. The TLE data is only available. The result is interesting: The In-Plane maneuvers showed more pronounced changes; The Out-of-Plane maneuvers showed detectable but less pronounced changes. Given the four graphs of each of North-South and East-West maneuvers, we believe that the (240 hours, 99%) pair also performed in this experiment, too.

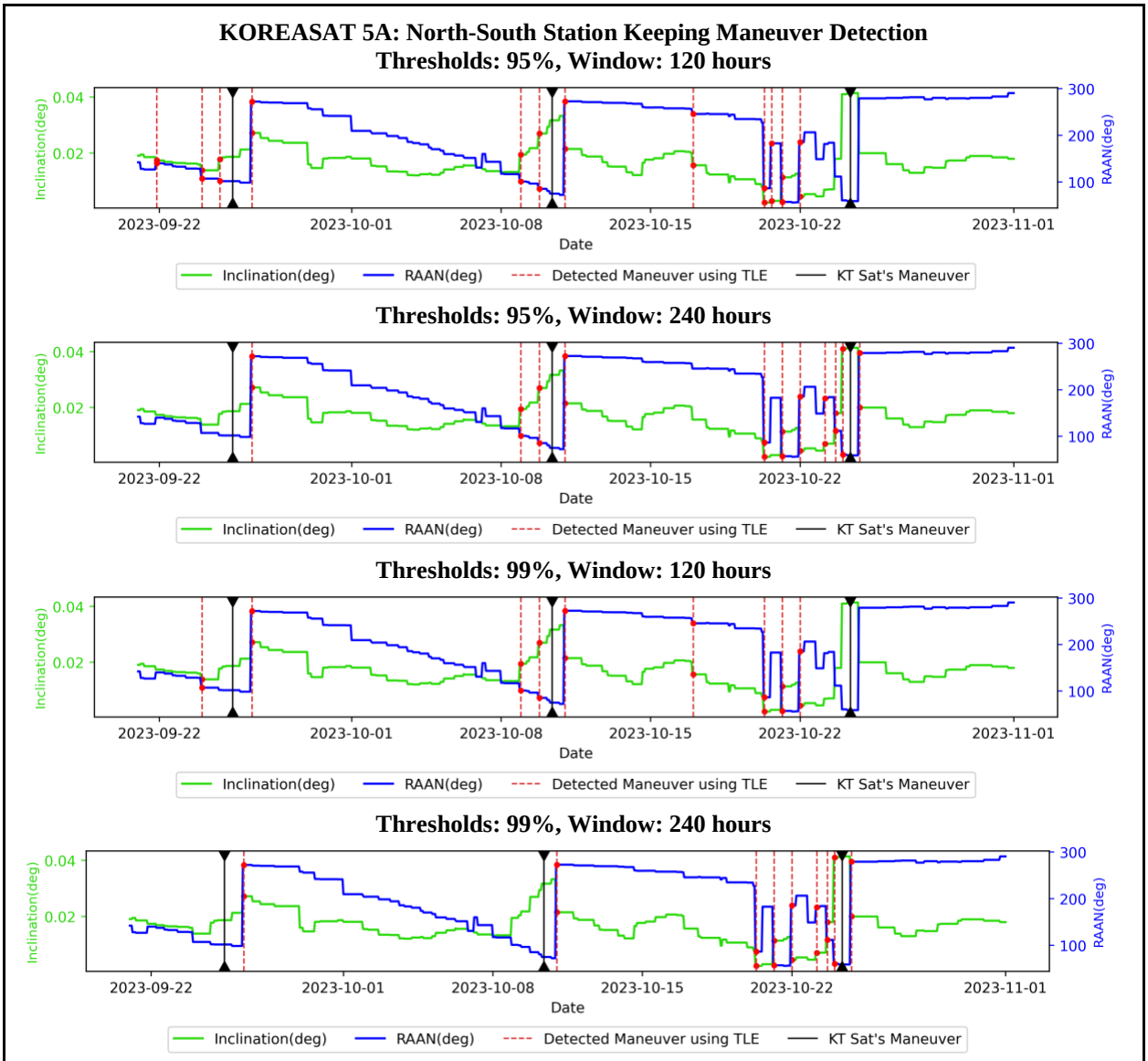

Fig. 9. KOREASAT 5A. Detecting North-South station-keeping maneuver. Period: 2023-09-21 ~ 2023-10-31. Black triangles correspond to the maneuvers performed by KT SAT. Red broken vertical lines correspond to the detected maneuvers. Each graph shows the intersection of detected maneuvers for both inclination and RAAN. This is to reduce false positive. The bottom-most (99%, 240 hours) case seems the best. Observe the detected maneuver moments are associated with latency from the actual maneuver. All computation done in a couple of seconds on an entry-level desktop computer.

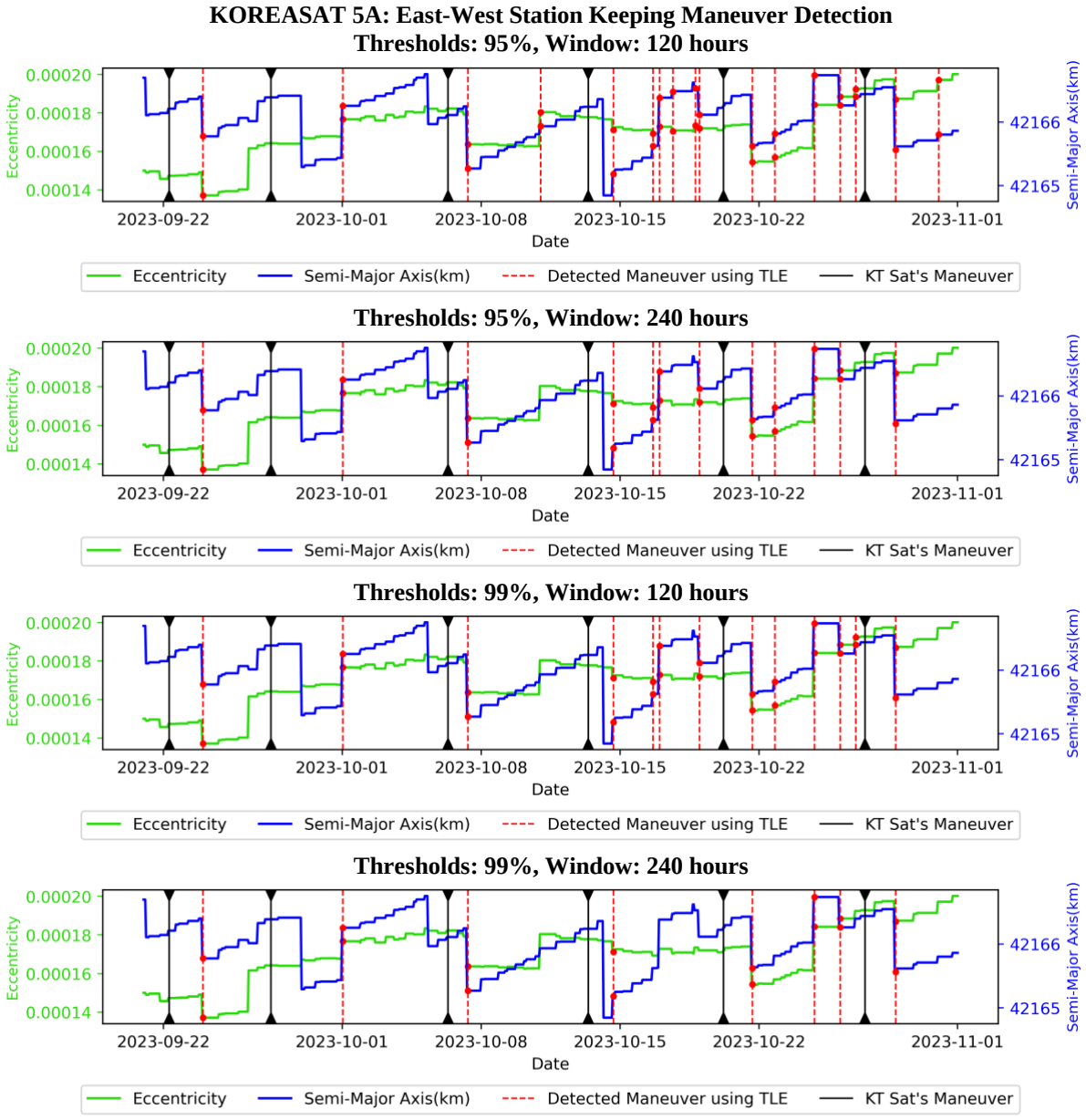

Fig. 10. KOREASAT 5A. Detecting East-West station-keeping maneuver. Period: 2023-09-21 ~ 2023-10-31. Black triangles correspond to the maneuvers performed by KT SAT. Red broken vertical lines correspond to the detected maneuvers. Each graph shows the intersection of detected maneuvers for both eccentricity and semi-major axis. This is to reduce false positive. The bottom-most (99%, 240 hours) case seems the best. Observe the detected maneuver moments are associated with latency from the actual maneuver. All computation done in a couple of seconds on an entry-level desktop computer.

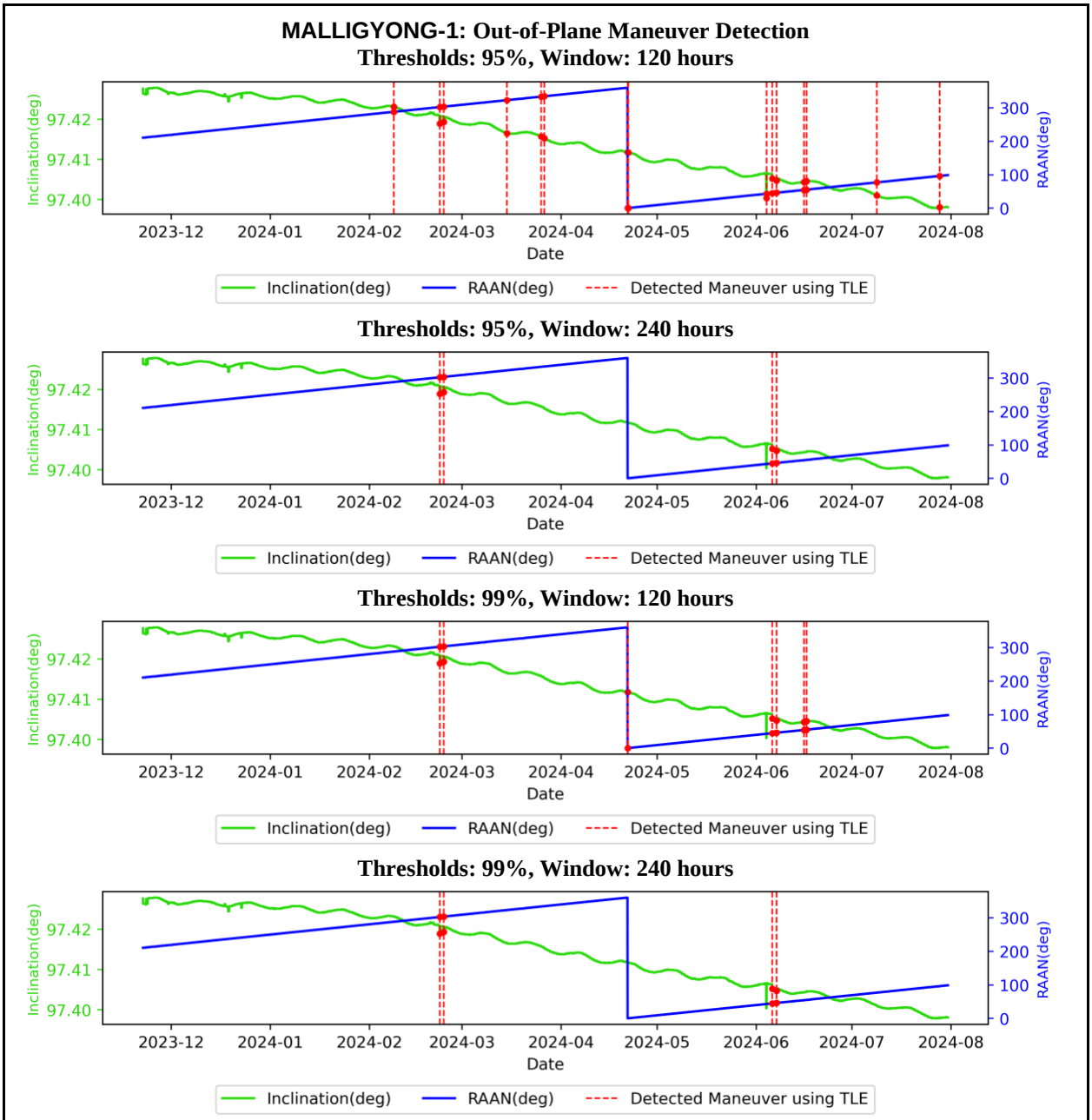

Fig. 11. MALLIGYONG-1. Detecting Out-of-Plane maneuver. Period: 2023-11-22 ~ 2024-07-31. Unlike K5A, the ground-truth maneuver time is not known. Red broken vertical lines correspond to the detected maneuvers. Each graph shows the intersection of detected maneuvers for both inclination and RAAN. This is to reduce false positive. The bottom-most (99%, 240 hours) case seems the best. All computation done in a couple of seconds on an entry-level desktop computer.

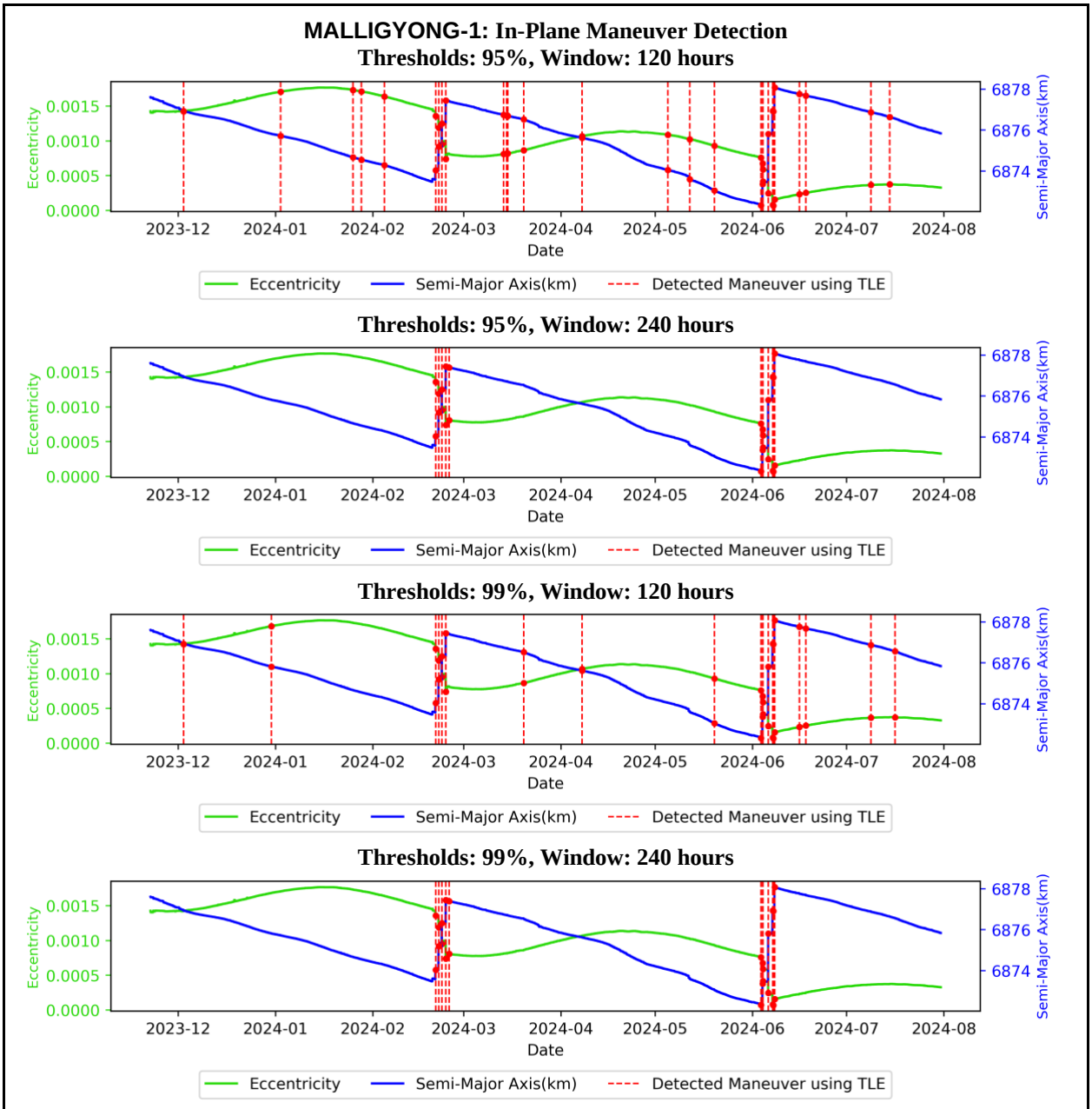

Fig. 12. MALLIGYONG-1. Detecting In-Plane maneuver. Period: 2023-11-22 ~ 2024-07-31. Unlike K5A, the ground-truth maneuver time is not known. Red broken vertical lines correspond to the detected maneuvers. Each graph shows the intersection of detected maneuvers for both eccentricity and semi-major axis. This is to reduce false positive. The bottom-most (99%, 240 hours) case seems the best. All computation done in a couple of seconds on an entry-level desktop computer.

7. Conclusion

Space is becoming more congested and contested. Applications in the New Space Age requires more accurate and efficient solutions to safety, optimization, and intelligence issues for space assets. Here we presented a rigorous case study on the efficiency and accuracy of the Space-Track TLE database compared to three sources of data: the CDM by the US Space Force, Safran, and KT SAT. We reconfirmed that the Space-Track TLE data was good and consistent with the CDM. We also observed that the latency of the TLE data was significant and must be accounted for as much as possible. We also presented an algorithm for early detection of maneuver using time series algorithms so that latency information could be used for better interpretation of the TLE data.

We proposed a concept of virtual meeting tool for SSA and STM where participants can be invited to share any space-situations including conjunctions and exchange different perspectives. We recommend that such a system has the capabilities of visualizing synchronized space-situations in addition to standard features of a virtual meeting platform for communicating using texts, voices, and videos. To have a concurrent avoidance negotiation capability, it is desirable to have the capability of generating and evaluating trajectory alternatives in real-time with respect to some measures, e.g., collision risks. We presented "42 Talks" as an example of such a platform for SSA and STM.

Acknowledgements
This research was supported by the National Research Foundation of Korea (NRF, Grant No. 2017R1A3B1023591), the Korea Institute of Startup and Entrepreneurship Development (KISED, Grant No. RS-2023-00283180), and the Institute for Information and Communication Technology Planning and Evaluation (IITP, Grant No. RS-2023-00259061).

References

[1] https://www.iarpa.gov/research-programs/sintra (accessed on August 31, 2024).
[2] Falle, Andrew, et al. "One million (paper) satellites." *Science* 382.6667 (2023): 150-152.
[3] Hoots, Felix R., Linda L. Crawford, and Ronald L. Roehrich. "An analytic method to determine future close approaches between satellites." *Celestial mechanics* 33.2 (1984): 143-158.
[4] https://spacenews.com/spacex-and-oneweb-spar-over-satellite-close-approach/ (accessed on August 31, 2024)
[5] Jehyun Cha, Joonghyun Ryu, Mokwon Lee, Chanyoung Song, Youngsong Cho, Schumacher, Paul, Misoon Mah, and Deok-Soo Kim. "DVD-COOP: Innovative Conjunction Prediction using Voronoi-filter based on the Dynamic Voronoi Diagram of 3D Spheres " (2017).
[6] Choi, S. S., Ryu, P. J., Sim, K., Seong, J., Song, J. W., Mah, M., & Kim, D. D. "AstroLibrary: A library for real-time conjunction assessment and optimal collision avoidance." *Journal of Space Safety Engineering* (2024).
[7] Lewis, Hugh G., and Georgia Skelton. "Safety considerations for large constellations of satellites." *Journal of Space Safety Engineering* (2024).
[8] Wilson, Cynthia, and Corey Best. "18 and 19 SDS Small Satellite Support." (2023).
[9] Decoto, Jacob, and Patrick Loerch. "Technique for GEO RSO station keeping characterization and maneuver detection." Advanced Maui Optical and Space Surveillance Technologies Conference. 2015.
[10] Inclan, Carla, and George C. Tiao. "Use of cumulative sums of squares for retrospective detection of changes of variance." *Journal of the American Statistical Association* 89.427 (1994): 913-923.
[11] Kim, Kyungwon, et al. "Unsupervised change point detection and trend prediction for financial time-series using a new cusum-based approach." *IEEE Access* 10 (2022): 34690-34705.
[12] Fahmy, Hany. "The rise in investors' awareness of climate risks after the Paris Agreement and the clean energy-oil-technology prices nexus." *Energy Economics* 106 (2022): 105738.
[13] Uçak, Harun, Esin Yelgen, and Yakup Arı. "The role of energy on the price volatility of fruits and vegetables: Evidence from Turkey." *Bio-based and Applied Economics Journal* 11.1 (2022): 37-54.
[14] Sansó, Andreu, J. L. Carrion, and V. Aragó. "Testing for changes in the unconditional variance of financial time series." *Revista de Economía Financiera*, 2004, vol. 4, p. 32-52 (2004).